IFSCC 2025 full paper (IFSCC2025-1498)

"Identification of Bioactive Compounds and Mechanistic Insights of Red Rice Extract in Skin Protection via AI-Enhanced System Pharmacology"

Yigang Chen [1,2,3,†], Tao Zhang [1,2,3,6,*], Ting-Syuan Lin [1,2,3,†], Xin Li [1,2,3], Xiang Ji [1,2,3], Shenghan Huang [1,2,3], Ziyue Zhang [1,2,3], Huali Zuo [1,2,3,4], Shangfu Li [1,2,3,4], Jing Li [1,2,3,4], Hsi-Yuan Huang [1,2,3,4], Yang-Chi-Dung Lin [1,2,3,4,*] and Hsien-Da Huang[1,2,3,4,5,*],

[1] School of Medicine, The Chinese University of Hong Kong, Shenzhen, Longgang District, Shenzhen, Guangdong 518172, China; [2] Warshel Institute for Computational Biology, +School of Medicine, The Chinese University of Hong Kong, Shenzhen, Longgang District, Shenzhen, Guangdong 518172, China; [3] Better Way Group - Chinese University of Hong Kong (Shenzhen) Warshel Joint Laboratory for skin health and active molecule innovation, Longgang District, Shenzhen, Guangdong 518172, China; [4] Guangdong Provincial Key Laboratory of Digital Biology and Drug Development, The Chinese University of Hong Kong, Shenzhen, Guangdong, P.R. China; [5] Department of Endocrinology, Key Laboratory of Endocrinology of National Health Commission, Peking Union Medical College Hospital, Chinese Academy of Medical Sciences & Peking Union Medical College, Beijing, 100730, P.R. China; [6] R&D center, Better Way (Shanghai) Cosmetics Co., Ltd., Shanghai, 201103, P.R. China; [†] These authors contributed equally to this work; [*] corresponding author.

Abstract

Taremi, a red rice extract, has demonstrated potential in mitigating photodamage, yet its bioactive components and mechanisms remain unclear. Here, we employed LC-MS to characterize its chemical composition, identifying 10 distinct compound classes via similarity network analysis. Using the SCOPE-DTI algorithm, we predicted target interactions for each class and constructed a photoaging-related target library. Integrative analysis revealed the regulatory strength of these compounds across six key pathways (oxidative stress, inflammation, mitochondria DNA repair, DNA damage, collagen, and melanin). Focusing on flavonoids as a representative class, we combined docking studies with a novel key compound-target prioritization method, uncovering synergistic roles of critical targets in antioxidant, anti-inflammatory, and DNA damage repair processes. Our findings systematically decode Taremi's polypharmacological effects, offering insights for natural product-based anti-photodamage strategies.

1. Introduction

Photoaging, the accelerated skin aging caused by chronic UV exposure, manifests as wrinkles, loss of elasticity, and hyperpigmentation [1]. Mechanistically, UV triggers excessive ROS production, leading to oxidative damage in proteins, lipids, and DNA—a key driver of skin degeneration [2] The ROS overaccumulation activates MAPK signaling, upregulating transcription factors NF-κB and AP-1. These factors coordinately induce HO-1 and MMPs, exacerbating oxidative stress and extracellular matrix degradation [2,3]. Activated NF-κB contributes to inflammation by upregulating the expression of pro-inflammatory mediators, including interleukin-8 (IL-8) and cyclooxygenase-2 (COX-2) [1]. The induction of heme oxygenase-1 (HO-1) may increase intracellular iron levels, which can, in turn, enhance the generation of reactive oxygen species (ROS) [2, 3]. Elevated levels of matrix metalloproteinases (MMPs) lead to the degradation of extracellular matrix proteins, contributing to wrinkle formation and potentially facilitating metastasis [2, 3].

To counteract UV-induced damage, antioxidants—particularly plant-derived compounds—have emerged as promising agents. Their ability to scavenge ROS and modulate oxidative stress-related pathways makes them ideal candidates for anti-photoaging interventions [4] Red rice (*Oryza sativa L*.), especially its bran layer, is a rich source of bioactive anthocyanins, flavonoids, and phenolic acids [5]. These compounds exhibit potent ROS-scavenging and anti-inflammatory activities, as demonstrated in UV-protection assays [6-8], positioning red rice as a viable material for anti-photoaging applications. Red rice bran extract has been utilized in skincare products (e.g., Taremi biological photo protection agent), yet its anti-photoaging efficacy is largely attributed to empirical observations rather than mechanistic insights. A major hurdle lies in deciphering how the complex chemical composition collectively modulates multiple targets—a systems-level understanding critical for rational formulation design but currently lacking.

Here, we systematically decode Taremi's anti-photoaging mechanism through a tripartite strategy: (1) LC-MS-based chemical profiling to identify key constituents, (2) SCOPE-DTI-driven target prediction to map compound-target interactions, and (3) pathway enrichment analysis to prioritize oxidative stress, inflammation, and DNA repair modules. Focusing on flavonoids,

we further validate their multi-target roles via molecular docking and a novel prioritization framework. Through in-depth analysis of flavonoids—validated by docking and a novel target prioritization framework—we demonstrate that Taremi's efficacy stems from the coordinated modulation of oxidative stress, inflammation, and DNA damage repair (Figure. 1). Beyond elucidating Taremi's polypharmacology, our study provides a translatable pipeline—from chemical characterization to pathway-level validation—that can accelerate the development of standardized natural extract-based cosmeceuticals.

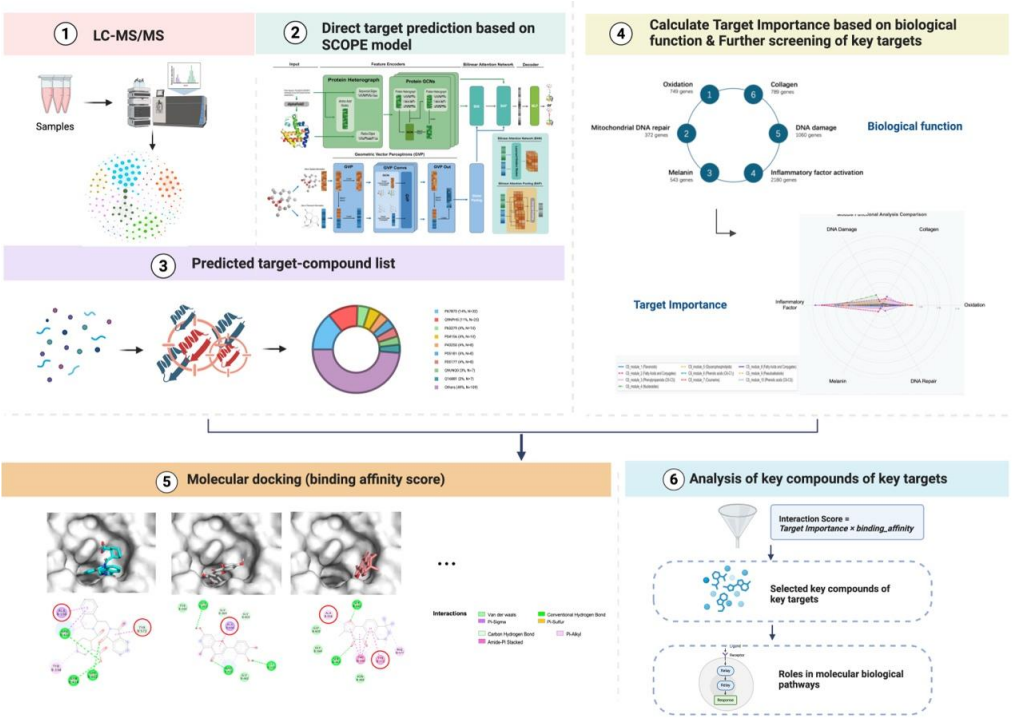

Figure 1. The workflow of this study.

2. Materials and Methods

LC-MS/MS analysis of Taremi

(1) Ultra-High Performance Liquid Chromatography (UHPLC): Shimadzu Nexera UHPLC LC-30A.

(2) Column: Shim-pack GIST 2 μm C18, 2.1 × 100mm, P/N: 227-30001-04; S/N: 21E 24484.

(3) Mass Spectrometry: TripleTOF 6600+, Sciex.

(4) Taremi samples: The TPFD sample was manufactured by Better Way (Shanghai) Cosmetics Co., Ltd., China (No. EPSP240924).

(5) Methanol was purchased from Fisher Chemical (A452-4; LOT: 218079).

(6) Ammonium Hydroxide was obtained from Fisher Scientific (No. A669-500).

(7) Ultra-pure water was prepared using the Direct-Q3 Water Purification System (Merck Millipore).

Chromatographic Conditions

Samples were analyzed using an UHPLC system coupled with an Sciex TripleTOF 6600+ mass spectrometer. Separation was performed on a C18 column (2 μm C18, 2.1 × 100mm). Mobile phase A was 99.9% water, and 0.01% ammonium hydroxide, while mobile phase B was 100% acetonitrile. Gradient elution was conducted with the following program: 0-2 min, from 0% to 5% B; 2-22 min, 99% B; 22-26 min, 99% B; 26-30 min, from 99% to 5% B. Flow rate: 0.3 mL/min; column temperature: 30°C; injection volume: 20 μL.

Mass Spectrometry Conditions

(1) Positive mode

Mass spectrometry analysis was performed using an Sciex TripleTOF 6600 Plus system with the following parameters: curtain gas (CUR) set to 35 psi, gas source 1 (GS1) at 55 psi, gas source 2 (GS2) at 55 psi, ion spray voltage (ISVF) at 5500 V, and ion source temperature (TEM) at 550°C.

(2) Negative mode

Mass spectrometry analysis was performed using an Sciex TripleTOF 6600 Plus system with the following parameters: curtain gas (CUR) set to 35 psi, gas source 1 (GS1) at 55 psi, gas source 2 (GS2) at 55 psi, ion spray voltage (ISVF) at -4500 V, and ion source temperature (TEM) at 550°C.

Preparation of reference compounds

Accurately weigh each reference standard and prepare a stock solution at a concentration of 1 mg/mL using methanol. Aliquots of each stock solution were precisely measured and combined to prepare a mixed standard solution using the initial mobile phase. The mixed solution was then diluted to concentration of 2.5 ug/mL.

Preparation of Taremi test solution

The sample was dissolved in 50% methanol to prepare a 10 mg/mL solution, followed by ultrasonication for 30 min. The mixture was then centrifuged at 20,000 × g for 20 min at 4°C. The supernatant was filtered through a 0.22 μm organic membrane filter, and the resultant filtrate was injected into the analytical system with an injection volume of 20 μL.

Compound similarity (CS) network

The compound similarity searches were conducted using RDkit based on molecular fingerprints. A compound similarity (CS) network was constructed, where the nodes represent individual compounds and the edges represent the relationships between them. Compounds with a Tanimoto coefficient (Tc) ≥ 0.5 were considered connected in the network, implying significant structural similarity. In the CS network, compounds are grouped based on their structural resemblance, where pairs of compounds with a Tc value of at least 0.5 are connected by an edge. To identify and separate the clusters within the CS network, the Louvain algorithm in Gephi was applied with a resolution of 1.0. Additionally, independent structural analyses were performed on the nodes (compounds) within each cluster using chemical data obtained from PubChem [9].

Pathway importance analysis

The calculation of functional dimension importance for each module follows a weighted approach that considers both protein importance and function prevalence. The core calculation process involves the following steps:

Each protein's importance is calculated using min-max normalization of its count value:

$$Importance(p) = \frac{Count(p) - Count_{min}}{Count_{max} - Count_{min}}$$

Where $Count(p)$ is the count value of protein p, and $Count_{max}$ and $Count_{min}$ are the minimum and maximum count values within that module.

For each functional dimension d, two factors are calculated:

$$WeightedSum(d) = \sum Importance(p)$$

$$\text{Prevalence}(d) = \frac{|P_d|}{|P|}$$

Where $|\mathrm{P_d}|$ is the number of proteins with function d, and $|P|$ is the total number of proteins in the module.

The final importance score for each dimension combines both factors:

$$\text{DimensionScore}(d) = \text{WeightedSum}(d) \times \text{Prevalence}(d)$$

This formula balances the importance of proteins having a particular function with how widespread that function is within the module. A function will score highly if it is associated with many important proteins.

Molecular Docking

Protein–ligand docking was conducted using AutoDock Vina (version 1.1.2) [10, 11], which utilizes a stochastic global optimization algorithm to estimate binding affinities and predict ligand conformations. Protein structures were preprocessed by removing crystallographic water molecules and adding polar hydrogens. Ligands were converted to docking-ready formats with proper protonation states using MGLTools (version 1.5.7) and Open Babel (version 3.1.0) [12]. Binding pockets were identified with P2Rank [13], a machine learning-based tool that detects ligandable cavities based on local geometric and physicochemical descriptors. The predicted pocket centers and dimensions were used to define the docking search space.

For each ligand–protein pair, multiple configurations were generated to specify the receptor, ligand, and docking box parameters. Docking simulations were executed in parallel batches, with AutoDock Vina producing multiple poses per complex, ranked by predicted binding free energy.

Following docking, the top-ranked pose from each run was extracted for analysis. These poses were then used to evaluate binding energy distributions and infer the most likely binding sites and orientations for each ligand.

3. Results

Construction of Compound Similarity Network Based on MS Identification of Taremi's Composition

A comprehensive collection of 261 compounds in Taremi was determined through mass spectrometry (MS) identification of its constituents. Among these, 209 compounds exhibit significant structural similarity. As shown in Figure 2A, the compound similarity (CS) network of Taremi was constructed using these 209 compounds. In this CS network, compounds are represented by nodes, and associations between pairs of compounds with a Tc value of 0.5 or higher are depicted as edges, indicating strong structural similarities between the connected compounds. The Louvain algorithm in Gephi (with a resolution of 1.0) was used to identify and separate clusters within the CS network. The structures of compounds within each cluster were analyzed individually using chemical data from PubChem. The CS network of Taremi, consisting of 209 nodes and 835 edges, was divided into 10 modules. Compounds within each module share a high degree of structural similarity, and the main constituents are summarized in Figure 2B.

These include flavonoids (module_1), fatty acids and conjugates (module_2), phenylpropanoids (C6-C3) (module_3), nucleosides (module_4), glycerophospholipids (module_5), phenolic acids (C6-C1) (module_6), and other bioactive compounds with diverse structures (others). The size of each node in the network is proportional to its degree, reflecting the importance of each compound within the network.

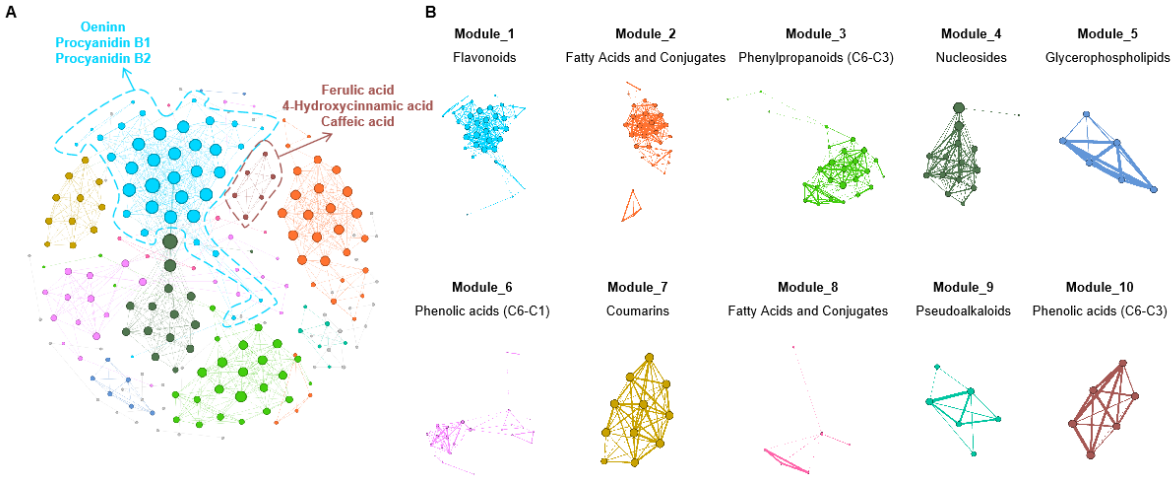

Figure 2. The CS network of Taremi. (A) CS network of Taremi was established based on 209 compounds. (B) Primary constituents of Taremi within each module exhibit substantial structural similarities.

Predict Compound Target by SCOPE-DTI

To further investigate the biological functions of each compound module in Taremi, we employed SCOPE-DTI, an advanced deep learning framework for drug-target interaction (DTI) prediction developed in our previous work. Designed to overcome the limitations of semi-inductive DTI prediction, SCOPE-DTI integrates three-dimensional structural representations with a bilinear attention network to effectively model cross-domain interactions (Figure 3). Unlike conventional methods constrained by sparse or imbalanced data, SCOPE-DTI leverages the largest well-annotated human DTI dataset, enabling robust predictions for novel compounds or targets. Its optimized architecture not only surpasses state-of-the-art approaches but also demonstrates strong practical applicability. The detailed methodology can refer to ref. arXiv:2503.09251.

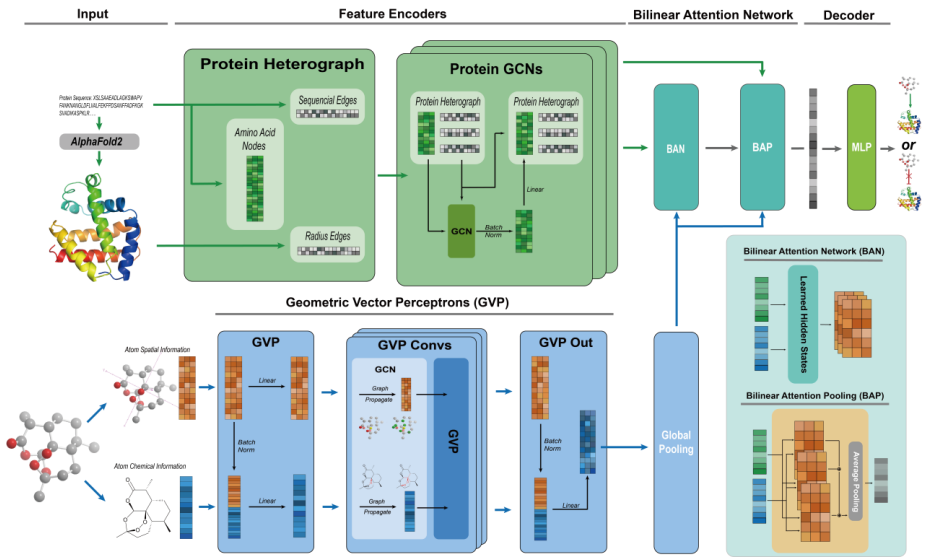

Figure 3. The deep learning algorithm framework of SCOPE-DTI.

Following SCOPE-DTI-based predictions, we analyzed the targets associated with each Taremi module (Figure 4). Notably, each module exhibited several key targets enriched across multiple small molecules, aligning with biological intuition—structurally similar compounds tend to share common targets. From a probabilistic perspective, targets frequently predicted across numerous molecules are more likely to be critically regulated, suggesting their functional importance within the respective module. This pattern was particularly pronounced in Module 1 (flavonoids), where the majority of compounds converged on a specific subset of targets, prompting further functional exploration of this module.

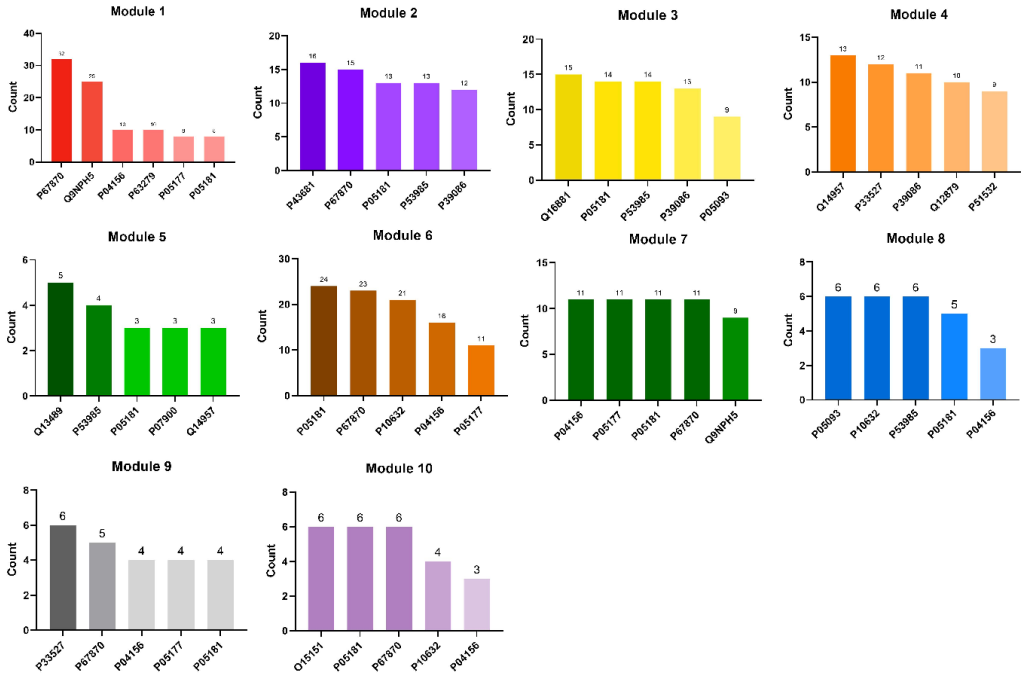

Figure 4. Distribution of top 5 prediction score rank counts across 10 compound similarity modules.

Functional Analysis of Taremi Modules Reveals Distinct Pathway Regulation Patterns

To systematically evaluate the biological relevance of each Taremi module, we first predicted protein targets using SCOPE-DTI and then performed functional annotation through MetaCore's comprehensive pathway-protein relationship database. Six key pathways related to photoaging and photodamage were analyzed: DNA damage, collagen metabolism, oxidation, DNA repair, melanin synthesis, and inflammatory factors.

The regulatory strength of each module was quantified through a two-tiered scoring system: (1) Protein importance scores were normalized within each module based on target prediction frequency (min-max scaling), and (2) Pathway-specific scores were derived by combining the weighted sum of normalized protein importance with the functional prevalence of targets in each pathway.

As illustrated in Figure 5, the radar chart reveals both shared and distinct functional profiles across modules. Most modules exhibited strong anti-inflammatory and antioxidant activities, consistent with Taremi's traditional medicinal uses. Notably, Module 1 (flavonoids) demonstrated exceptional functional specificity—its regulatory effects were almost exclusively confined to anti-inflammatory and antioxidant pathways, with minimal activity in other dimensions. This remarkable selectivity aligns with our earlier finding that Module 1 compounds converge on a narrow set of high-confidence targets (Figure 4), suggesting a mechanistically coherent mode of action.

Several modules (e.g., Module 4 and 9) showed broader pathway engagement, including collagen protection and DNA repair, indicating their potential as multi-functional photoprotective agents. The nucleoside-rich Module 4 uniquely prioritized DNA damage response pathways, highlighting the value of our modular analysis in identifying specialized biological functions.

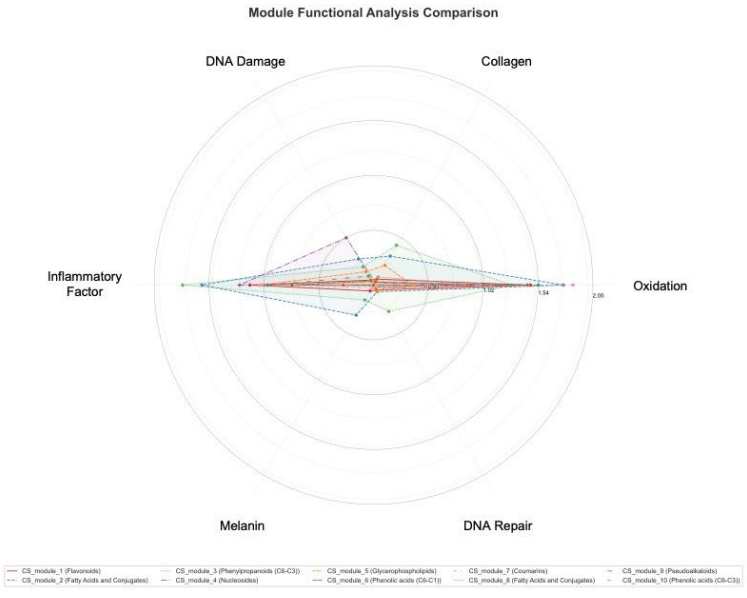

Figure 5. Pathway importance score for each module on six photoaging pathophysiology related pathways.

Key Compounds and Key Targets Identification

We systematically evaluated the interaction efficacy between key targets and bioactive compounds in module 1 by employing a dual-quantitative framework integrating target importance and interaction scores. Target importance was calculated through a normalization formula based on the frequency of compound-target interactions within the module, while interaction scores were defined as the product of target importance (p) and docking scores, enabling prioritized ranking of critical compounds.

$$\text{Interaction Score} = \text{Target Importance (p)} \times |\text{binding\_affinity}|$$

The results demonstrated that the top three prioritized targets in Module 1 were P67870 (target importance: 1), Q9NPH5 (0.774), and P63279 (0.290), with their corresponding core compounds identified as Vicenin-3, Diosmin, Procyanidin B2, Oenin, and Procyanidin B1. Vicenin-3, a plant-derived metabolite implicated in antioxidative, anti-inflammatory, and disease-resistant pathways, exhibited functional relevance to metabolic regulation in plant systems. Diosmin, a natural flavonoid compound, displayed pronounced vasoprotective, antioxidative, and anti-inflammatory properties. Procyanidin B2, Oenin, and Procyanidin B1, belonging to the proanthocyanidin class of flavonoids, demonstrated multifaceted bioactivities, including antioxidative effects, anti-inflammatory responses, and cardiovascular protective mechanisms (Table 1). This analytical framework provides quantitative validation for the polypharmacological activities associated with both the target cluster in module 1 and their corresponding compounds, establishing a prioritized basis for further mechanistic exploration and therapeutic optimization.

Table 1. Top three prioritized targets in Module 1 interaction score with key compounds.

PubChem_ID	Name	Uniport_ID	Target _importance	Binding _affinity	Interaction _score
185958	Vicenin-3	P67870	1	10.8	10.8
5281613	Diosmin		1	10.8	10.8
443652	Oenin		1	9	9
185958	Vicenin-3	Q9NPH5	0.8	13.9	10.8
5281613	Diosmin		0.8	13.9	10.8
122738	Procyanidin B2		0.8	12.8	9.9
443652	Oenin		0.8	10.6	8.2
5281613	Diosmin	P63279	0.3	9.9	2.9
122738	Procyanidin B2		0.3	9.6	2.8
185995	Vicenin-3		0.3	8.8	2.6
443652	Oenin		0.3	8.2	2.4
11250133	Procyanidin B1		0.3	6.7	1.9

4. Discussion

The IKK/NF-κB pathway is a central hub in inflammation, tightly regulated through multiple upstream signals and post-translational modifications [14]. Casein kinase 2 (CK2) has emerged as a pivotal modulator within this cascade, promoting the phosphorylation of IκBα both directly and via activation of the IKK complex. Phosphorylation of IκBα triggers its proteasomal degradation, leading to the release and nuclear translocation of NF-κB. In parallel, CK2 phosphorylates Ser529 on the p65 subunit of NF-κB, enhancing its transcriptional activity. Environmental stimuli such as particulate matter (PM2.5) can further potentiate this axis. In keratinocytes, ligation of Toll-like receptor 5 (TLR5) by PM2.5 induces NADPH oxidase 4 (NOX4)-mediated reactive oxygen species (ROS) production, which activates NF-κB and drives the expression of pro-inflammatory cytokines, including IL-6 [15].

In response to genotoxic stress, a distinct regulatory layer of NF-κB activation is orchestrated through sumoylation. ATM kinase, likely in coordination with poly(ADP-ribose) polymerase 1 (PARP1), promotes the sumoylation of nuclear NEMO and RIPK1. These modifications facilitate their cytoplasmic translocation and subsequent ubiquitylation, enabling the formation of a TAK1-containing complex that activates the IKK complex via phosphorylation of IKKα and IKKβ. This pathway is self-limiting through NF-κB-induced expression of the SUMO protease SENP2, which desumoylates NEMO, thereby halting further signal propagation [16].

Downstream of NF-κB, ROS and pro-inflammatory cytokines initiate a broader transcriptional program via RTK-Ras-MAPK pathways, including the activation of AP-1, STAT1/3, and HIF-1, as well as TGF-β signaling. These converging axes orchestrate a robust inflammatory response, linking extracellular stress to nuclear transcriptional reprogramming [17].

Here, we identify several natural compounds capable of modulating key nodes in this network. Vicenin-3 (Vi, 185958) and Diosmin (Di, 5281613) concurrently target CK2, NOX4, and SUMO, suggesting a multifaceted anti-inflammatory potential. Procyanidin B2 (PB2, 122738) and Oenin (Oe, 443652) act on NOX4 and SUMO, while Procyanidin B1 (PB1, 11250133) specifically modulates SUMO-dependent signaling. These compounds collectively reduce oxidative stress, inflammation, and DNA damage, offering promising candidates for therapeutic intervention in inflammation-associated pathologies (Figure. 6).

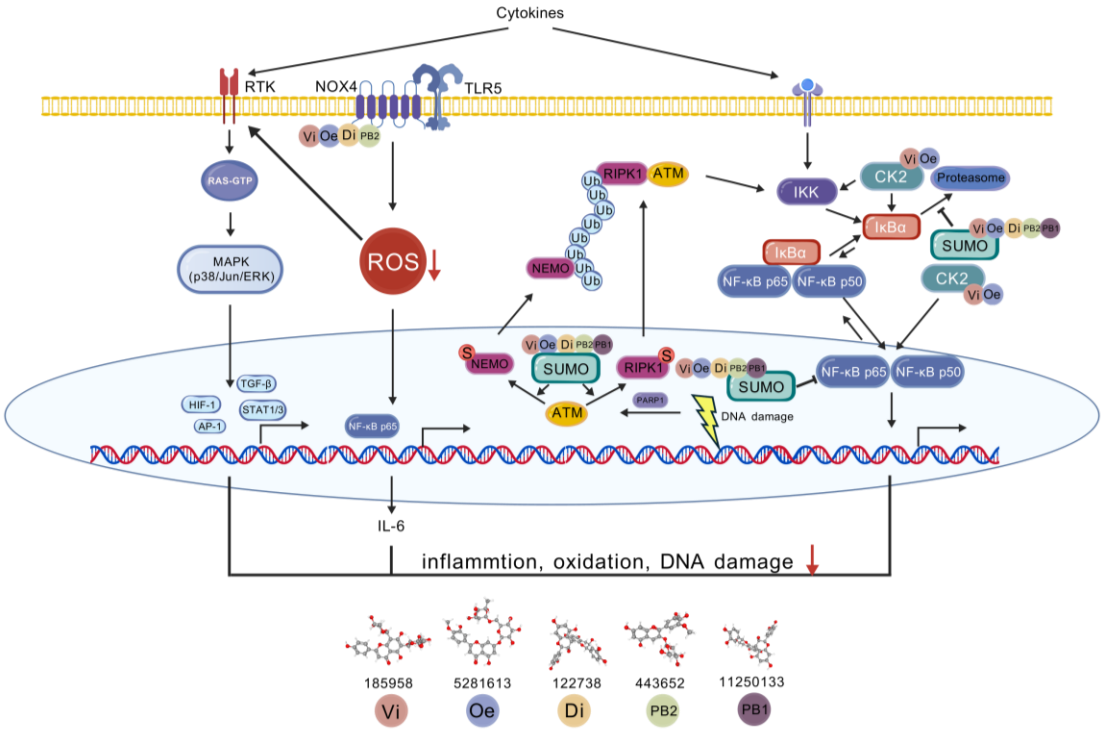

Figure 6. Taremi's activate compounds modulate of the CK2–NOX4–SUMO axis attenuates inflammation and oxidative stress.

5. Conclusion

This study systematically elucidates the active constituents of Taremi and their multi-target mechanisms against photoaging, bridging a critical gap in understanding natural extract-based interventions. Through an integrative approach combining LC-MS phytochemical profiling, SCOPE-DTI target prediction, and pathway enrichment analysis, we reconstructed the multi-target network of Taremi's ten bioactive classes, spanning oxidative stress, inflammation, and DNA damage repair pathways. Focusing on proanthocyanidins as a representative class, we employed molecular docking and a novel target prioritization algorithm to demonstrate their synergistic regulation of: (1) ROS scavenging via NOX4 inhibition, (2) NF-κB-mediated anti-inflammatory effects, and (3) SUMO-dependent DNA repair enhancement. Furthermore, we identified several natural compounds, such as Vicenin-3 and Diosmin, that modulate key nodes in the network, including CK2, NOX4, and SUMO, thereby exhibiting significant anti-inflammatory potential. Other compounds like Procyanidin B2 and Oenin also target NOX4 and SUMO, while Procyanidin B1 specifically influences SUMO-dependent signaling. Collectively, these compounds contribute to the reduction of oxidative stress, inflammation, and DNA damage, these findings position Taremi-derived compounds as promising leads for inflammation-asso-

ciated dermatopathies. Beyond photoaging, our established pipeline—from phytochemical deconvolution to multi-omics target mapping—offers a blueprint for rational development of standardized botanical therapeutics in skincare and beyond.

References

1. Chen, X., C.S. Yang, and G. Jiang, *Research progress on skin photoaging and oxidative stress.* Postepy Dermatologii I Alergologii, 2021. **38**(6): p. 931-936.
2. Saewan, N. and A. Jimtaisong, *Natural products as photoprotection.* Journal of Cosmetic Dermatology, 2015. **14**(1): p. 47-63.
3. Cooper, S.J. and G.T. Bowden, *Ultraviolet B regulation of transcription factor families:: Roles of nuclear factor-kappa B (NF-κB) and activator protein-1 (AP-1) in UVB-induced skin carcinogenesis.* Current Cancer Drug Targets, 2007. **7**(4): p. 325-334.
4. Zhang, T., et al., *Mechanistic Insights into Pigmented Rice Bran in Mitigating UV-Induced Oxidative Stress, Inflammation, and Pigmentation.* Cosmetics 2025, Vol. 12, Page 51, 2025. **12**(2): p. 51-51.
5. Kothapalli, L., et al., *Nutritional and Medicinal Value of Red Rice.* Current Traditional Medicine, 2023. **9**(6).
6. Sinthorn, W., et al., *Thai red rice extract provides liver protection in paracetamol-treated mice by restoring the glutathione system.* Pharmaceutical Biology, 2016. **54**(5): p. 770-779.
7. Yakaew, S., et al., *Hom-Kularb-Dang rice bran extract for the prevention of UVB-damage against human skin fibroblast.* Chiang Mai University Journal of Natural Sciences, 2020. **19**(1): p. 34-51.
8. Zhang, T., et al., *Red jasmine rice bran extract for the prevention of the blue light induced photodamges.* Frontiers in Medical Science Research, 2024. **6**(4): p. 67-71.
9. Zuo, H.L., *An analytical method of pathway-based target networks and its application in modern research of herbal formulae*. 2020, University of Macau: Macau.
10. Trott, O. and A.J. Olson, *AutoDock Vina: improving the speed and accuracy of docking with a new scoring function, efficient optimization, and multithreading.* J Comput Chem, 2010. **31**(2): p. 455-61.
11. Morris, G.M., et al., *AutoDock4 and AutoDockTools4: Automated docking with selective receptor flexibility.* J Comput Chem, 2009. **30**(16): p. 2785-91.
12. O'Boyle, N.M., et al., *Open Babel: An open chemical toolbox.* J Cheminform, 2011. **3**: p. 33.
13. Krivak, R. and D. Hoksza, *P2Rank: machine learning based tool for rapid and accurate prediction of ligand binding sites from protein structure.* J Cheminform, 2018. **10**(1): p. 39.
14. Borgo, C., et al., *Protein kinase CK2: a potential therapeutic target for diverse human diseases.* Signal Transduct Target Ther, 2021. **6**(1): p. 183.
15. Ryu, Y.S., et al., *Particulate matter induces inflammatory cytokine production via activation of NFκB by TLR5-NOX4-ROS signaling in human skin keratinocyte and mouse skin.* Redox Biol, 2019. **21**: p. 101080.
16. Seeler, J.-S. and A. Dejean, *SUMO and the robustness of cancer.* Nature Reviews Cancer, 2017. **17**(3): p. 184-197.

17. Rudolf, J., et al., *NADPH Oxidases and Their Roles in Skin Homeostasis and Carcinogenesis.* Antioxid Redox Signal, 2018. **28**(13): p. 1238-1261.